

Exploration of the intrinsic inertial response of ferroelectric domain walls via molecular dynamics simulations

Shi Liu, Ilya Grinberg, and Andrew M. Rappe

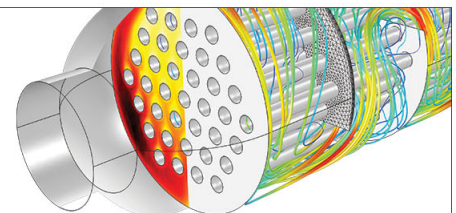
Citation: [Applied Physics Letters](#) **103**, 232907 (2013); doi: 10.1063/1.4832421

View online: <http://dx.doi.org/10.1063/1.4832421>

View Table of Contents: <http://scitation.aip.org/content/aip/journal/apl/103/23?ver=pdfcov>

Published by the [AIP Publishing](#)

Over **700** papers &
presentations on
multiphysics simulation



VIEW NOW ►

 COMSOL

Exploration of the intrinsic inertial response of ferroelectric domain walls via molecular dynamics simulations

Shi Liu, Ilya Grinberg, and Andrew M. Rappe^{a)}

The Makineni Theoretical Laboratories, Department of Chemistry, University of Pennsylvania, Philadelphia, Pennsylvania 19104-6323, USA

(Received 26 July 2013; accepted 31 October 2013; published online 5 December 2013)

The motion of ferroelectric domain walls (DWs) is critical for various applications of ferroelectric materials. One important question that is of interest both scientifically and technologically, is whether the ferroelectric DW has significant inertial response. To address this problem, we performed canonical ensemble molecular dynamics simulations of 180° and 90° DWs under applied electric fields. Examination of the evolution of the polarization and local structure of DWs reveals that they stop moving immediately after the removal of electric field. Thus, our computational study shows that ferroelectric DWs do not have significant intrinsic inertial response. © 2013 AIP Publishing LLC. [<http://dx.doi.org/10.1063/1.4832421>]

Ferroelectric materials have been studied intensely due to their numerous important technological applications in electronics, optics, and acoustics.^{1–4} In many cases, ferroelectrics adopt a multi-domain state where domains with polarization uniformly oriented in one direction are bounded by domains with polarization pointing in other directions. The boundary separating regions of different polarity is called the domain wall (DW).¹ The DW can be moved by external electric field and stress, causing one region to grow. Therefore, controlling DW motion is critical to applications of ferroelectric materials such as non-volatile random access memory.^{5–8} Though ferroelectric materials have been studied for more than fifty years, the microscopic understanding of how different types of DWs form and move remains incomplete.

One unanswered question that is of interest both scientifically and technologically, is whether ferroelectric DWs exhibit real momentum and significant inertial response. It is generally reported that a ferroelectric DW, the motion of which involves movements of atoms, has real inertia, whereas the magnetic DW, which is due to the flipping of massless spins, has no momentum.^{9,10} However, these claims have been challenged recently for both ferroelectric and magnetic DWs.^{11–14} For magnetic domains, experimental studies reveal that magnetic DWs can exhibit significant momentum and inertial response.^{13,14} For ferroelectrics, the inertial response of a DW can be evaluated by examining its behavior after the driving force is removed. This effect is currently a subject of debate. Dawber *et al.*¹⁵ observed that the ferroelectric DW travels ballistically from the perimeter to the center in a circular capacitor: once the wall motion is initiated, it propagates with viscous drag, which they attributed to the coupling of the domain wall to acoustic phonons. The good agreement between the measured dependence of impedance response on capacitor perimeter and theoretical predictions with a simple one-dimension phonon drag equation suggests that the ferroelectric DW has significant inertial response. Similar deceleration of the DW under applied field

was observed by Kim *et al.*¹⁶ and also assigned to the ballistic character of DW motion. However, Molotskii *et al.*¹¹ later pointed out that Dawber *et al.* used a high value for the relaxation time ($\tau \approx 50$ ns). After using a much smaller τ ($\approx 10^{-4}$ ns) derived from the effective DW mass reported by Kittel,¹⁷ Molotskii *et al.* obtained a post-field propagation distance around 10^{-10} m, which is smaller than the lattice constant.¹¹ Furthermore, recent *in-situ* investigations of the dynamics of superdomain (*a-c* domain bundles) boundaries in BaTiO₃ with piezoresponse force microscopy (PFM) also indicated that the DW stops when the external voltage is turned off.¹² The presence or lack of momentum of DWs can have both extrinsic and intrinsic origins. To elucidate the *intrinsic* inertial response, we perform molecular dynamics (MD) simulations of ferroelectric DWs.

To model the dynamics of DWs, the simulation of a large system at finite temperature is required. We have recently developed an interatomic potential based on bond-valence theory.^{18–23} The model potentials for two ferroelectric materials, PbTiO₃ and BiFeO₃, have been parameterized based on first-principles results.^{22,23} The optimized potential is accurate for both constant volume (*NVT*) and constant pressure (*NPT*) conditions and sufficiently efficient for large-scale ($\approx 1\,000\,000$ atoms) MD simulations. In this work, we use MD simulations to study the momentum of DWs in the classic PbTiO₃ ferroelectric. As shown in Figure 1, the 180° DW (the wall separating regions with antiparallel polarization) is constructed with a $24 \times 8 \times 8$ supercell with polarization aligned along *z* axis. The 90° DW (the wall separating regions with perpendicular polarization) is modeled with a $40 \times 40 \times 40$ supercell with alternating domains having polarization in the *xy* plane.

We perform *NPT* MD simulations with a Parrinello-Rahman barostat as follows: first, the DW motion is initiated by applying an external electric field for a period of time; then the field is turned off allowing the DWs to evolve freely. If the DW does indeed have momentum, it will keep moving after the electric field is removed. Given that accurate determination of the DW position is critical for the evaluation of momentum, we first determined the thickness of DWs. As shown in Figure 2, we calculated the averaged

^{a)} Author to whom correspondence should be addressed. Electronic mail: rappe@sas.upenn.edu.

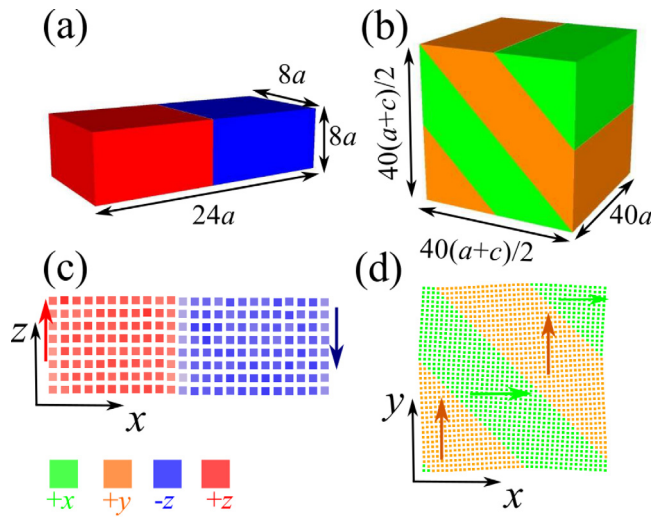


FIG. 1. Domain walls in PbTiO_3 . (a) $24 \times 8 \times 8$ supercell used for 180° DW. (b) $40 \times 40 \times 40$ supercell used for 90° DW. (c) Domain pattern of 180° DW in the xz plane. (d) Domain pattern of 90° DW in the xy plane. Each cell is colored based on the direction of the dipole: green for $+x$, orange for $+y$, red for $+z$, and blue for $-z$.

polarization for each layer of cells across the DWs at temperatures from 10 K to 240 K. We found that the 180° DW is 1–2 unit cells thick, while the width of 90° DW is 4–5 unit cells (the half width of the polarization profile around the domain boundary) at finite temperature. In this study, we propose that only when a DW moves inertially by a distance comparable to the width of a DW, can the inertial response be regarded as “significant.”

The change of the overall polarization of the supercell directly reflects the DW motion. Figure 3 presents the change of P_z for 180° DW under various pulses at 220 K. As the electric field is applied along $+z$ direction, the magnitude of P_z increases, indicating the field-driven movement of DW along $+x$. Once the field is turned off, two types of equilibrations are observed: (1) the magnitude of P_z is reduced until it reaches equilibrium, for example, for $E = 1.8$ MV/cm, $t_E = 4$ ps; (2) the magnitude of P_z first decreases, then increases by a small amount and eventually equilibrates, for example, $E = 2.2$ MV/cm, $t_E = 4$ ps. To elucidate the origins of these two types of equilibrations, we examined the

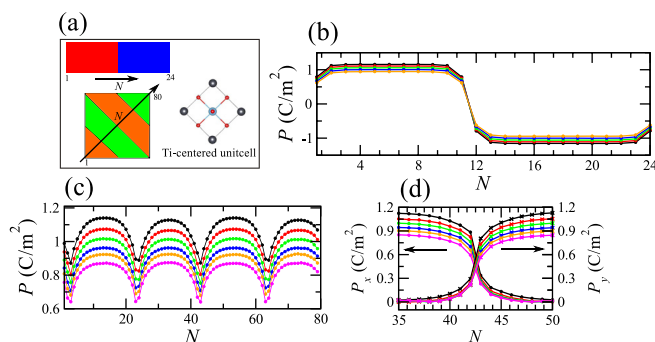


FIG. 2. (a) Illustration of our choice of layer index, N , in DWs. The Ti-centered unit cell is used for local polarization calculation. (b) and (c) Temperature-dependent polarization profiles across the 180° DW and the 90° DW. (d) Temperature-dependent x -component and y -component polarization profiles across the 90° DW from layer $N = 35$ to layer $N = 50$. Lines with different color represent different temperatures: black, 10 K; red, 100 K; green, 160 K; blue, 200 K; orange, 220 K; and magenta, 240 K.

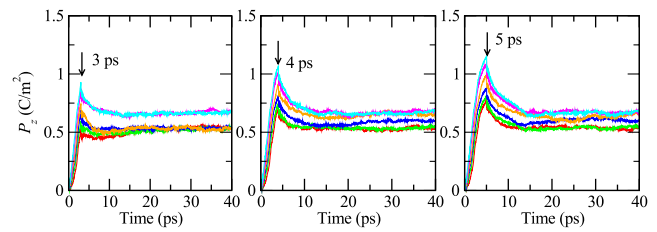


FIG. 3. The evolution of z -component polarization of 180° DW in response to electric field pulse. Lines with different color represent different electric fields: red, 1.8 MV/cm; green, 2.0 MV/cm; blue, 2.2 MV/cm; orange, 2.4 MV/cm; magenta, 2.6 MV/cm; and cyan, 2.8 MV/cm. The electric field is turned off at 3 ps, 4 ps, and 5 ps, respectively.

structure of 180° DW by analyzing the evolution of the local polarizations in the supercell. Figure 4 presents the change of the polarization profile in response to a 4 ps-long electric field pulse. The drop of P_z at the instant of field removal results mainly from the reduction in the magnitudes of local dipoles that were aligned with the applied field ($+z$) and the increase in the magnitude of the dipoles pointing toward $-z$. When the field is removed, both types of dipoles return to their zero-field values. More importantly, both the polarization profiles and the visualized domain patterns show that the position of the DW does not change once the field is removed, which suggests that the 180° DWs do not have inertial response. The two types of polarization responses are actually caused by the growth or annihilation of a nucleus at the domain boundary. At 4 ps, we see from Figure 4(a) that the local dipoles in layer $N = 16$ are partially switched at the time of field removal. Similarly, in Figure 4(b), it is observed that the switching process in layer $N = 16$ has already started, but has not yet finished. This means the domain wall is not flat during the motion. Figure 5 shows the changes of the dipoles in these two layers in the absence of electric field. We can see that at 4 ps, the nucleus (number of red squares) in $N = 16$ ($E = 1.8$ MV/cm) is small and eventually disappears, resulting in the reduction of the polarization (Type 1 response). This is consistent with experimentally observed backswitching of the domain boundary after the driving

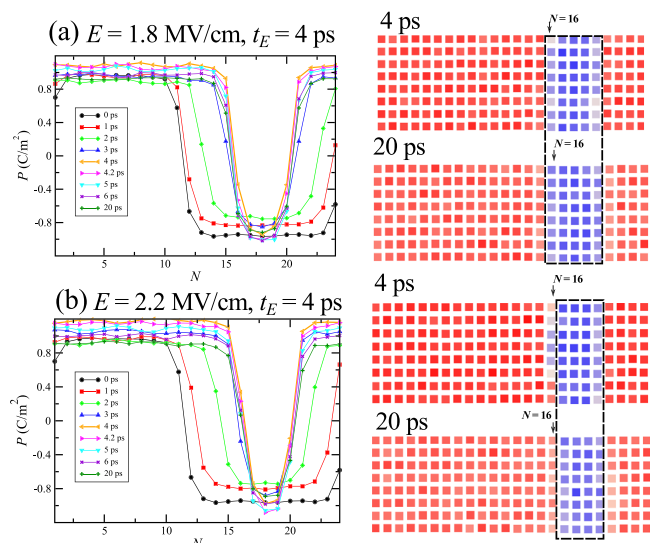


FIG. 4. Evolution of the polarization profiles (left) and domain patterns (right) of a 180° DW in PbTiO_3 .

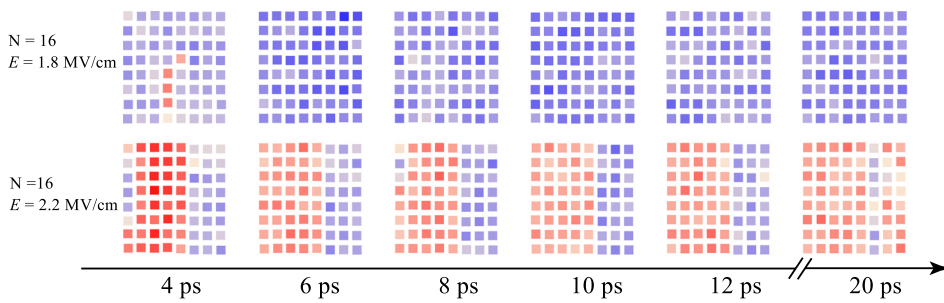


FIG. 5. Schematic representation of nucleus annihilation (top) and growth (bottom) at domain boundary. The electric field is turned off at 4 ps.

electric field is removed.¹² On the other hand, the size of nucleus in layer $N=16$ ($E=2.2$ MV/cm) is already large; therefore, the nucleus can keep growing until the whole layer becomes $+z$ polarized. This spontaneous switching process is responsible for the increase of the polarization (Type 2 response). We therefore suggest that after the electric field is turned off, only the layers in which the size of nucleus exceeds the critical size will finish the switching process in the absence of electric field. The cessation of DW motion at the instant of field-removal is a direct consequence of the intrinsic energy barrier for nucleation. We would like to note here the difference between a phonon and a DW. The motion of a phonon and a DW both involve the displacements of atoms. However, phonons are distortions away from a *single* local minimum in the structural phase space; displacing one atom creates forces on its neighbors, leading to the propagation of a phonon wave. By contrast, when a ferroelectric bicrystal is at rest, atoms are located in *one of the two* local minima ($+z$ or $-z$ domain) and are not under any force. A traveling DW, as we showed, moves one plane of atoms from one local minimum ($-z$ domain) to another local minimum ($+z$ domain). Therefore, during DW motion there is no restoring force that would cause the atoms in nearby unit cells to switch the direction of their off-center ferroelectric distortion.

The experimental studies cited above^{12,15,16} have found that the DW velocity under applied field is time-dependent and the speed of DW at a given time depends on the initial velocity and damping. However, according to Merz's law, DW velocity depends only on the strength of the applied field at the given time.²⁵ To investigate whether there is any memory of previous conditions in the intrinsic DW motion mechanism, we carried out two sets of simulations. In one set of simulations, the DWs are initially driven by electric fields of different magnitudes and then the field magnitudes are changed to the same value for all simulations. In another set of simulations, the same electric field is applied initially for all simulations, followed by the application of different electric fields. Figure 6 shows the time evolution of the polarization obtained by using this protocol in *NVT* simulations with a $48 \times 8 \times 8$ supercell. The slope of the polarization profile, k , specifies the speed of the DW. As shown in Figure 6(a), the DWs that experience a higher initial field show larger velocities before 6 ps. For $t > 6$ ps, the field is set to the same value for all simulations, all DWs show nearly identical velocities, regardless of their initial launching velocities. The dramatic difference in the velocities before and after 6 ps is illustrated in the insert of Figure 6(a). From Figure 6(b), we find that the velocities of DWs under

different fields follow Merz's law, $\ln v \propto 1/E$.²⁵ Our simulations show that the velocity of the DW does not depend on the initial velocity and has no time dependence, dissimilar to a ballistic motion. Instead, the velocity follows Merz's law and is solely dependent on the magnitude of the external electric field. This further demonstrates that the 180° DW has little or no intrinsic inertial response.

We now examine the 90° DWs. The evolution of P_x for 90° DW in response to different electric-field pulses at 200 K is shown in Figure 7. Since the 90° DW energy is known to be about four times lower than the 180° DW energy,²⁴ much smaller electric fields were applied along $+x$ direction. The increased magnitude of x -component of total polarization under electric field again indicates the movement of DWs driven by field. Similar to what was found for 180° DWs, the removal of electric field results in a decrease of P_x . Figure 8 shows the changes of domain patterns and P_x profiles for a 4 ps 0.4 MV/cm electric pulse. The motion of 90° DW (highlighted as red broken line) is evident from 0 ps to 4 ps. The overall result is an increase of the area of field-favored domains at the expense of the domains with dipoles oriented opposite to the field. After the field is turned off, the positions of the DWs from 4 ps to 20 ps did not change (Figure 8(b)), suggesting that 90° DW also does *not* have physically meaningful intrinsic inertial response. The main effect after the field removal is the structural relaxation leading to reduction of the x -component polarizations.

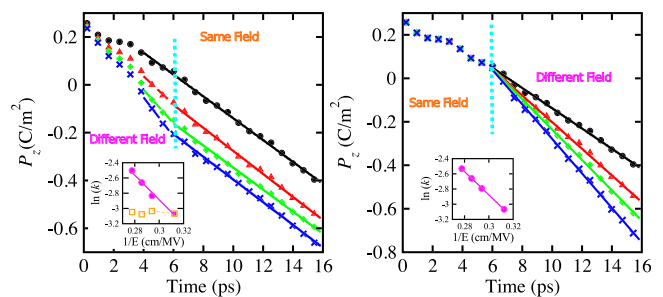


FIG. 6. Evolution of the polarization of a 180° DW under sequentially applied electric fields of different magnitudes. The electric field is applied along $-z$ direction. Symbols with different colors represent different electric fields: black, 3.2 MV/cm; red, 3.4 MV/cm; green, 3.5 MV/cm; and blue, 3.6 MV/cm. For a given electric field, 20 simulations starting with different initial equilibrated structures are performed to get the averaged polarization profile. (a) Different electric fields are applied until 6 ps and then switched to the same electric field (3.2 MV/cm). The inset illustrates the dependence on the DW velocity on the initial applied field for $t < 6$ ps (magenta) and $t > 6$ ps (orange). (b) The electric fields of the same magnitude (3.2 MV/cm) are applied until 6 ps and then switched to different electric fields. The inset shows that the speed of a DW follows Merz's law.

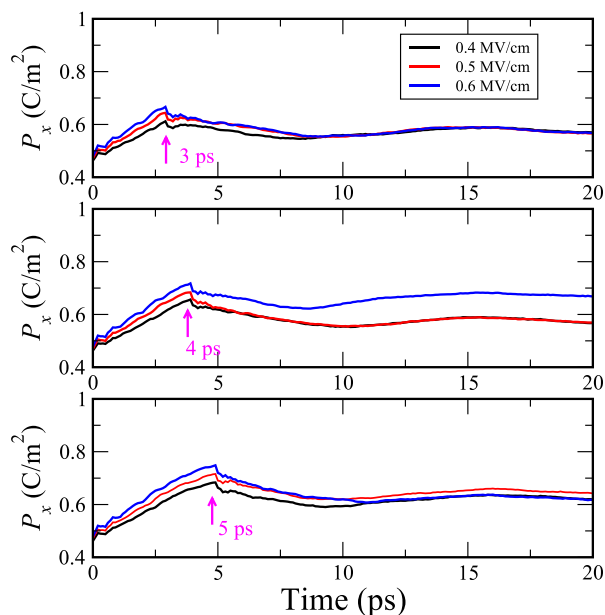


FIG. 7. The evolution of x -component polarization 90° DW in response to electric pulse. The electric field is turned off at 3 ps, 4 ps, and 5 ps, respectively.

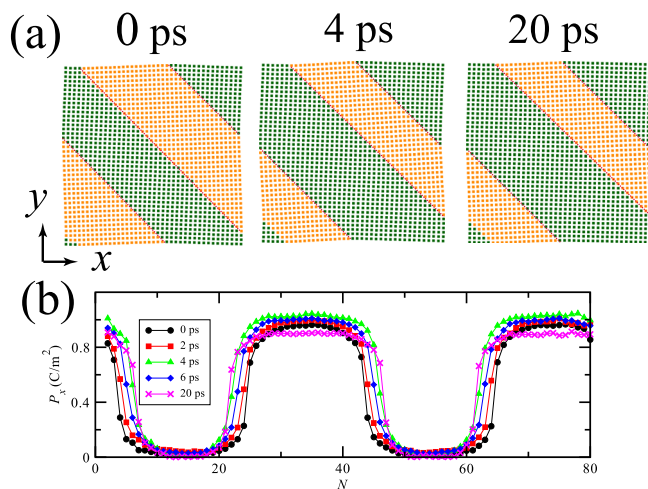


FIG. 8. Evolution of (a) the domain patterns and (b) polarization profiles of a 90° DW experiencing 4 ps 0.4 MV/cm electric pulse.

In summary, we have explored the motions of both 180° and 90° domain walls in PbTiO_3 , subjecting multi-domain samples to electric field pulses via molecular dynamics simulations. The analysis of changes of polarization and evolution of domain patterns reveal that both types of domain walls stop moving when the electric field is turned off and show that the velocity is solely determined by the strength of the electric field at any given time. We therefore conclude that

ferroelectric domain walls do not exhibit significant intrinsic inertial response. Inertial movement found in previous experiments is therefore likely to be driven by extrinsic effects (e.g., stress).

S.L. was supported by the NSF through Grant DMR11-24696. I.G. was supported by the US DOE under Grant DE-FG02-07ER46431. A.M.R. was supported by the US ONR under Grant N00014-12-1-1033. Computational support was provided by the U.S. DOD through a Challenge Grant from the HPCMO and by the U.S. DOE through computer time at NERSC. We thank Professor Marty Gregg for stimulating discussions.

¹M. E. Lines and A. M. Glass, *Principles and Applications of Ferroelectrics and Related Materials* (Clarendon Press, Oxford, 1977).

²J. F. Scott, *Ferroelectric Memories* (Springer, Berlin, 2000).

³J. F. Scott, *Science* **315**, 954 (2007).

⁴K. Rabe, Ch. H. Ahn, and J.-M. Triscone, *Physics of Ferroelectrics: A Modern Perspective*, Topics in Applied Physics Vol. 105 (Springer, Berlin, 2007).

⁵S. M. Yang, J. Y. Jo, D. J. Kim, H. Sung, T. W. Noh, H. N. Lee, J.-G. Yoon, and T. K. Song, *Appl. Phys. Lett.* **92**, 252901 (2008).

⁶T. H. Kim, S. H. Baek, S. M. Yang, S. Y. Jang, D. Ortiz, T. K. Song, J.-S. Chung, C. B. Eom, T. W. Noh, and J. G. Yoon, *Appl. Phys. Lett.* **95**, 262902 (2009).

⁷J. Seidel, L. W. Martin, Q. He, Q. Zhan, Y. H. Chu, A. Rother, M. E. Hawkrige, P. Maksymovich, P. Yu, M. Gajek, N. Balke, S. V. Kalinin, S. Gemming, F. Wang, G. Catalan, J. F. Scott, N. A. Spaldin, J. Orenstein, and R. Ramesh, *Nature Mater.* **8**, 229 (2009).

⁸H. Lu, C.-W. Bark, D. Esque de los Ojos, J. Alcala, C. B. Eom, G. Catalan, and A. Gruverman, *Science* **336**, 59 (2012).

⁹G. Catalan, J. Seidel, R. Ramesh, and J. F. Scott, *Rev. Mod. Phys.* **84**, 119 (2012).

¹⁰J. F. Scott, *ISRN Mater. Sci.* **2013**, 1–25.

¹¹M. Molotskii, Y. Rosenwaks, and G. Rosenman, *Annu. Rev. Mater. Res.* **37**, 271 (2007).

¹²P. Sharma, R. G. P. McQuaid, L. J. McGilly, J. M. Gregg, and A. Cruverman, *Adv. Mater.* **25**, 1323 (2013).

¹³L. Thomas, M. Hayashi, X. Jiang, R. Moriya, C. Rettner, and S. Parkin, *Science* **315**, 1553 (2007).

¹⁴L. Thomas, R. Moriya, C. Rettner, and S. S. P. Parkin, *Science* **330**, 1810 (2010).

¹⁵M. Dawber, D. J. Jung, and J. F. Scott, *Appl. Phys. Lett.* **82**, 436 (2003).

¹⁶Y. Kim, H. Han, W. Lee, S. Baik, D. Hesse, and M. Alexe, *Nano Lett.* **10**, 1266 (2010).

¹⁷C. Kittel, *Phys. Rev.* **83**, 458 (1951).

¹⁸I. D. Brown, *Chem. Rev.* **109**, 6858 (2009).

¹⁹I. Grinberg, V. R. Cooper, and A. M. Rappe, *Nature* **419**, 909 (2002).

²⁰Y.-H. Shin, V. R. Cooper, I. Grinberg, and A. M. Rappe, *Phys. Rev. B* **71**, 054104 (2005).

²¹Y.-H. Shin, I. Grinberg, I.-W. Chen, and A. M. Rappe, *Nature* **449**, 881 (2007).

²²S. Liu, I. Grinberg, and A. M. Rappe, *J. Phys.: Condens. Matter* **25**(1–6), 102202 (2013).

²³S. Liu, I. Grinberg, H. Takenaka, and A. M. Rappe, *Phys. Rev. B* **88**, 104102 (2013).

²⁴B. Meyer and D. Vanderbilt, *Phys. Rev. B* **65**, 104111 (2002).

²⁵W. J. Merz, *Phys. Rev.* **95**, 690–698 (1954).